JNS 1 (2012) 44-53

Journal of
NANOSTRUCTURES
JNS
NANOSTRUCTURES
JNS.kashanu.ac.ir

Laminar mixed convection of Cu-water nano-fluid in two-sided lid-driven enclosures

G. A. Sheikhzadeh, N. Hajialigol [*], M. Ebrahim Qomi, A. Fattahi

Department of Mechanical Engineering, University of Kashan,Ghotb Ravandi Blvd, Kashan, 87317-51167, Iran.

Article history:
Received 10/10/2011
Accepted 18/12/2011
Published online 1/1/2012

Keywords:
Lid-driven enclosure
Laminar mixed convection
Nanofluid
Aspect ratio

**Corresponding author:*
E-mail address:
Najmeh.hajialigol@gmail.com

Abstract

The fluid flow and heat transfer in lid-driven enclosures filled with Cu-water nanofluid is numerically investigated. The moving vertical walls of the enclosure are maintained in a constant temperature, while the horizontal walls are insulated. The hybrid scheme is used to discretize the convection terms and SIMPLER algorithm is adopted to couple the velocity field and pressure in the momentum equations. The effect of moving direction of walls on mixed convection is studied for various Ri numbers, aspect ratios and volume fractions of nanoparticles. For this purpose, vertical walls are moved in two directions: one, force convection aids to free convection and two, it interacts to free convection. It is observed that the direction of moving wall mainly affected the flow field, temperature gradient and heat transfer. In addition, by increasing the volume fraction of nanoparticles, the variation of average Nusselt number on the hot wall, as an index of heat transfer rate, is linear in two cases.

1. Introduction

Convection heat transfer is a chiefly applicable method regarding to engineering systems such as electronic equipment, solar collectors, heat exchangers, heating and cooling equipment. But, low thermal properties of working fluids are a main limitation. Suspending different types of small solid particles in conventional fluids is a functional means of improving the heat transfer performance

of common fluids which have low thermal properties. The dispersed particles in a base fluid called nanofluid are first used by Choi [1].

Nomenclature

Ar	Aspect ratio	X, Y	Dimensionless of Cartesian coordinates
g	Gravitational acceleration	**Greek symbols**	
Gr	Grashof number	α	Thermal diffusivity
H	Enclosure height	β	Fluid thermal expansion coefficient
L	Enclosure length	φ	Solid volume fraction
Nu	Nusselt number	μ	Dynamic viscosity
k_f	Thermal conductivity of the fluid	υ	Kinematics viscosity
k_s	Thermal conductivity of the solid	ρ	Density
p	Pressure	θ	Dimensionless temperature
P	Dimensionless pressure	**Subscript**	
Pr	Prandtl number	avg	average
Re	Reynolds number	c	Cold wall
Ri	Richardson number	eff	Effective
T	Temperature	f	Fluid
u, v	Components of velocity	h	Hot wall
U, V	Dimensionless of velocity component	nf	Nanofluid
V_p	Velocity of the moving lid	s	Solid
x, y	Cartesian coordinates		

Among the numerous geometry studied in the heat transfer of nanofluids, the lid-driven enclosure has been a subject of interest in recent years due to its applications especially those related to lubrication technologies, electronic cooling, food processing and nuclear reactors [2-3]. Thus, many studies have been performed to investigate natural convection in a lid-driven enclosure using a working nanofluid.

Luo and Yang [4] presented a continuation method to calculate flow field with and without heat transfer in a two-sided lid-driven enclosure with an aspect ratio of 1.96. The top and bottom lids of the enclosure move in opposite directions. Al-Amiri et al [5] simulated steady mixed convection in a square lid-driven enclosure for a fluid of Pr = 1 using the Galerkin weighted residual method. They showed that heat transfer characteristics of flow are increased for low values of the Richardson numbers due to the mechanical induced effect of the moving lid. Ghasemi and Aminossadati [6] investigated mixed convection in a lid-driven triangular enclosure filled with a water-Al_2O_3 nanofluid. The effects of parameters such as Richardson number, solid volume fraction and the direction of the sliding wall motion were studied. It was indicated that the downward wall motion leads to a stronger vortexes within the enclosure and a higher heat transfer rate. Talebi et al. [7] numerically studied mixed convection in a square lid-driven enclosure using a copper-water nanofluid. The Reynolds number was varied between 1 and 100 and the solid volume fraction between 0 and 0.05. It is found that the effect of volume fraction on the flow pattern and thermal behavior is more noticeable at a higher Rayleigh number.They also concluded that the effect of volume fraction variation decreases with increasing Reynolds number. Mansour et al. [8] investigated mixed convection flows in a partially heated lid-driven square enclosure utilizing nanofluids. According to their results, adding alumina nanoparticles (Al_2O_3) to the base fluid (water) gives larger values of Nusselt number, while adding titanium oxide nanoparticles (TiO_2) to the base fluid gives smaller values of Nusselt number.

Abu-Nada and Chamkha [9] studied steady laminar mixed convection flow in a lid-driven inclined square enclosure filled with water-Al_2O_3 nanofluid. They surveyed the effects of the presence of nanoparticles and enclosure inclination angle on the flow and heat transfer. They found that heat transfer is accentuated by inclination of the enclosure at moderate and large Richardson numbers.

In this study, a lid-driven enclosure is considered to investigate mixed convection. The vertical isothermal walls are slid in two directions: one, forced convection aids free convection and two, forced convection interacts with free convection. Streamlines, isotherms and heat transfer are investigated in several aspect ratios of the enclosure for pure water and Cu-water nanofluid.

2. Physical model and governing equations

A schematic diagram of the enclosure with coordinate system and boundary conditions is shown in Fig. 1. The vertical lids have different constant temperatures. The horizontal walls are assumed to be insulated. Two different cases are considered as shown in the figure. In case I, the left wall (cold wall) is moving up, while the right wall (hot wall) is moving down. In case II, the left wall is moving down while the right wall is moving upwards. The moving walls have the same velocity in two cases. The gravitational force direction is parallel to the moving walls.

The enclosure is filled with a Newtonian nanofluid. The nanoparticles are assumed to have uniform shape and size. Also, it is assumed that both the fluid phase and nanoparticles are in the thermal equilibrium state and flow with the same velocity in laminar regime. The physical properties of the nanofluid are considered to be constant except the density which varies according to the Boussinesq approximation.

Under the above assumptions, the steady-state two-dimensional governing equations are:
Continuity equation:

$$\frac{\partial u}{\partial x}+\frac{\partial v}{\partial y}=0 \tag{1}$$

x-momentum equation:

$$u\frac{\partial u}{\partial x}+v\frac{\partial u}{\partial y}=-\frac{1}{\rho_{nf}}\frac{\partial p}{\partial x}+\frac{\mu_{nf}}{\rho_{nf}}\left(\frac{\partial^2 u}{\partial x^2}+\frac{\partial^2 u}{\partial y^2}\right) \tag{2}$$

y-momentum equation:

$$u\frac{\partial v}{\partial x}+v\frac{\partial v}{\partial y}=\frac{-1}{\rho_{nf}}\frac{\partial p}{\partial y}+\frac{\mu_{nf}}{\rho_{nf}}\left(\frac{\partial^2 v}{\partial x^2}+\frac{\partial^2 v}{\partial y^2}\right)+\frac{1}{\rho_{nf}}g(\rho\beta)_{nf}(T-T_c) \tag{3}$$

Energy equation:

$$\mathrm{u}\frac{\partial \mathrm{T}}{\partial \mathrm{x}}+\mathrm{v}\frac{\partial \mathrm{T}}{\partial \mathrm{y}}=-\frac{1}{\rho_{\mathrm{nf}}}\frac{\partial \mathrm{p}}{\partial \mathrm{y}}+\alpha_{\mathrm{nf}}\left(\frac{\partial^2 \mathrm{T}}{\partial \mathrm{x}^2}+\frac{\partial^2 \mathrm{T}}{\partial \mathrm{y}^2}\right) \tag{4}$$

Where

$$\alpha_{\mathrm{nf}}=\frac{\mathrm{k_{eff}}}{(\rho \mathrm{c_p})_{\mathrm{nf}}}$$

and the effective viscosity of nanofluid as given by Brinkman [10] is:

$$\mu_{\mathrm{nf}}=\frac{\mu_{\mathrm{f}}}{(1-\varphi)^{2.5}} \tag{5}$$

The effective density of nanofluid at reference temperature is:

$$\rho_{\mathrm{nf}}=(1-\varphi)\rho_{\mathrm{f}}+\varphi\rho_{\mathrm{s}} \tag{6}$$

and the specific heat capacity of nanofluid is:

$$(\rho\beta)_{nf} = (1-\varphi)(\rho\beta)_f + \varphi(\rho\beta)_s \quad (7)$$

$$(\rho c_p)_{nf} = (1-\varphi)(\rho c_p)_f + \varphi(\rho c_p)_s \quad (8)$$

as given by Xuan and Li [11]. Here, φ is the volume fraction of nanoparticles, and the subscripts f, nf and s stand for base fluid, nanofluid and solid, respectively.

The effective thermal conductivity of a fluid can be determined by Maxwell-Garnett's [12] approximation model. For the two-component spherical-particle suspension, the model gives:

$$\frac{k_{nf}}{k_f} = \frac{(k_s + 2k_f) - 2\varphi(k_f - k_s)}{(k_s + 2k_f) + \varphi(k_f - k_s)} \quad (9)$$

Using the dimensionless variables

$$X = \frac{x}{H} \quad Y = \frac{y}{H} \quad U = \frac{u}{V_p} \quad V = \frac{v}{V_p}$$

$$P = \frac{p}{\rho {V_p}^2} \qquad \theta = \frac{T - T_c}{T_h - T_c}$$

the governing equations are written in the dimensionless form:

Continuity equation:

$$\frac{\partial U}{\partial X} + \frac{\partial V}{\partial Y} = 0 \quad (10)$$

x-momentum equation:

$$U\frac{\partial U}{\partial X} + V\frac{\partial U}{\partial Y} = -\frac{\rho_f}{\rho_{nf}}\frac{\partial P}{\partial X} + \frac{1}{\vartheta_f Re}\frac{\mu_{nf}}{\rho_{nf}}\left(\frac{\partial^2 U}{\partial X^2} + \frac{\partial^2 U}{\partial Y^2}\right) \quad (11)$$

y-momentum equation:

$$U\frac{\partial V}{\partial X} + V\frac{\partial V}{\partial Y} = -\frac{\rho_f}{\rho_{nf}}\frac{\partial P}{\partial Y} + \frac{1}{\vartheta_f Re}\frac{\mu_{nf}}{\rho_{nf}}\left(\frac{\partial^2 V}{\partial X^2} + \frac{\partial^2 V}{\partial Y^2}\right) + \frac{(\rho\beta)_{nf}}{\beta_f \rho_{nf}} Ri\theta \quad (12)$$

Energy equation:

$$U\frac{\partial \theta}{\partial X} + V\frac{\partial \theta}{\partial Y} = \frac{\alpha_{nf}}{\alpha_f}\frac{1}{PrRe}\left(\frac{\partial^2 \theta}{\partial X^2} + \frac{\partial^2 \theta}{\partial Y^2}\right) \quad (13)$$

The Grashohf, Reynolds, Richardson and Prandtl numbers in the above equations are defined as:

$$Gr = \frac{g\beta H^3 (T_h - T_c)}{{\vartheta_f}^2} \qquad Re = \frac{V_p H}{\vartheta_f}$$

$$Ri = \frac{Gr}{Re^2} \qquad Pr = \frac{\vartheta_f}{\alpha_f}$$

Dimensionless boundary conditions are as follow:

$$\text{at } X = 0\ , \quad 0 \le Y \le 1 \ : \begin{Bmatrix} U = 0 \\ V = 1 \text{ or } V = -1 \\ \theta = 0 \end{Bmatrix}$$

$$\text{at } X = 1\ , 0 \le Y \le 1 \ : \begin{Bmatrix} U = 0 \\ V = -1 \text{ or } V = 1 \\ \theta = 1 \end{Bmatrix}$$

$$\text{at } Y = 0\ , 0 \le X \le 1 \ : \begin{Bmatrix} U = V = 0 \\ \frac{\partial \theta}{\partial Y} = 0 \end{Bmatrix}$$

$$\text{at } Y = 1\ , 0 \le X \le 1 \ : \begin{Bmatrix} U = V = 0 \\ \frac{\partial \theta}{\partial Y} = 0 \end{Bmatrix}$$

Nusselt number on the vertical hot wall is calculated as follows:

$$Nu = \frac{-k_{eff}}{k_f}\frac{\partial\theta}{\partial X}\Big|_{X=1} \quad (14)$$

Finally, the average Nusselt number is determined from:

$$Nu_{avg} = \int_0^1 Nu(y)dy \quad (15)$$

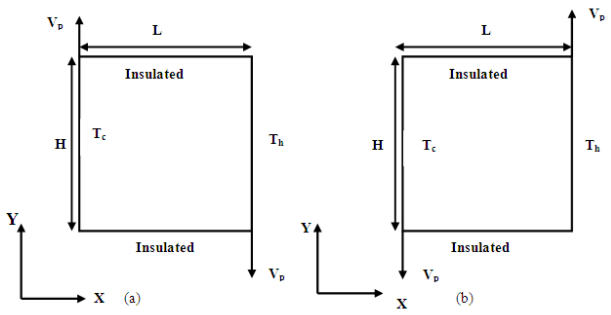

Fig. 1. Physical model and co-ordinates for two cases: (a) Case I; (b) Case II.

3. Numerical method

The governing non-linear equations together with the boundary conditions were solved by iterative numerical method using the finite volume technique. The hybrid scheme, which was a combination of the central difference scheme and the upwind scheme, was used to discretize the convection terms. A staggered grid system, in which the velocity components were stored midway between the scalar storage locations, was used. In order to couple the velocity field and pressure in the momentum equations, the well-known SIMPLER (semi-implicit method for pressure-linked equations revised) algorithm was adopted. Grid independency test was performed for a sample case. The set of linear algebraic equations was solved using TDMA (Three Diagonal Matrix Algorithm). The under-relaxation factors for U-velocity, V-velocity, and energy equations were chosen 0.3, 0.3, and 0.5, respectively. The convergence criterion of the numerical method was chosen as the total normalized.

3.1. Code Validation

In this study, the non-uniform grid which is finer in vicinity of verticals walls has been used in order to increase the accuracy of the results. To reach grid independency, the various grids (21×21, 41×41, 61×61 and 81×81) have been tested for φ=0.08 and Ri = 10.

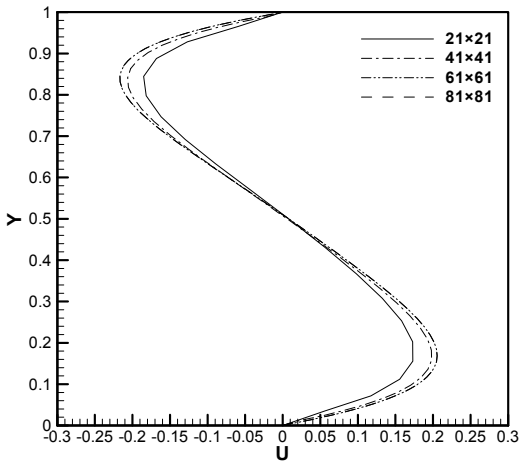

Fig. 2. Grid independence test for case I, Ri = 10, Ar = 1 and φ = 0.08: x-velocity distribution in the vertical mid-plane.

Fig. 2 shows U-velocity profile in the vertical mid-plane. Based on the figure, the grid size of 61×61 is adequately appropriate and economical to ensure a grid independent solution.

Fig. 3 presents comparison between the present results and those of Talebi et al. [7]. It is obvious that two sets of results coincide with good accuracy. In addition, Table 1 compares the average Nusselt number on the hot wall obtained by the present study with that of some previous studies in the similar problem.

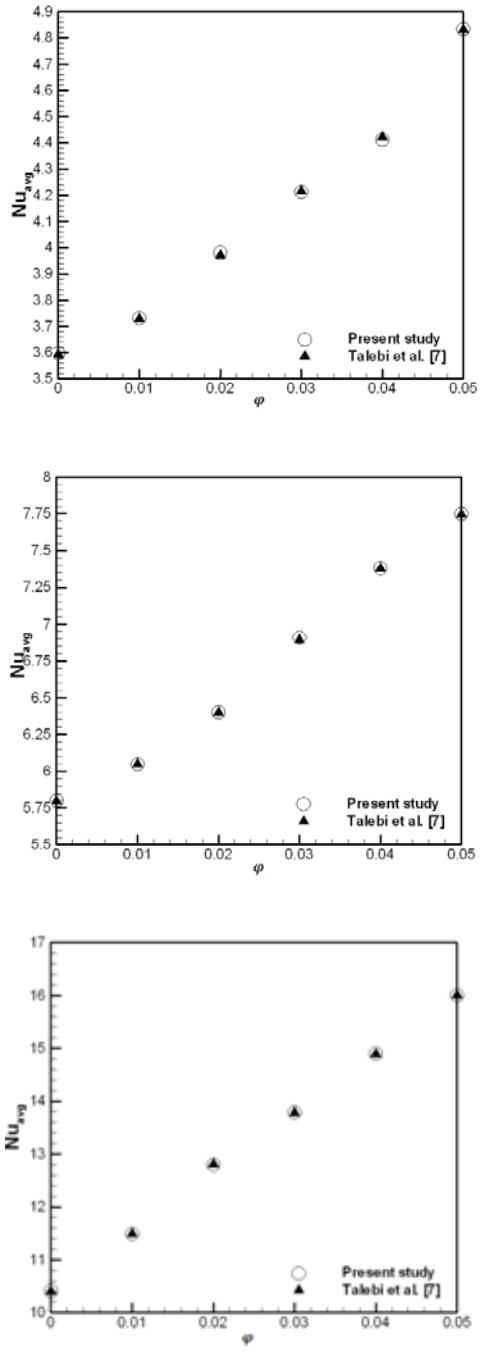

Fig. 3. Average Nusselt number on the cold wall: comparison between the present results and results of Talebi et al. [7]

Although there are some differences, the obtained results are in good agreement with the reference results.

Table 1. Average Nusselt number on the hot wall: comparison between the present work and data of some previous references.

	$Ra=10^3$	$Ra=10^4$	$Ra=10^5$	$Ra=10^6$
Present work	1.125	2.242	4.514	8.79
Khanafer et al [13]	1.118	2.245	4.522	8.826
Barakos and Mitsoulis [14]	1.114	2.245	4.51	8.806
Markatos and Pericleous [15]	1.108	2.201	4.43	8.754
De Vahl Davis [16]	1.118	2.243	4.519	8.799
Fusegi et al [17]	1.052	2.302	4.646	9.012

4. Results and discussion

The present study is carried out for pure-water and copper-water nanofluid. The aspect ratio, Ar, considered as the ratio of H/L takes three different values: 0.25, 1.0 and 4.0. The Richardson number, Ri, is varied as 0.1, 1, and 10. To vary Ri, Grashof number is fixed at Gr = 104. The thermo physical properties of fluid and solid are shown in Table 2. The discussion is established on two cases: Case I and Case II. In case I, the left wall is moving upwards while the right wall moves downwards. In case II, the vertical walls are moving in opposite direction of case I.

Fig. 4 shows streamlines and isotherms for various aspect ratios and Ri numbers for both nanofluid (Cu-water) and pure water as the base fluid in case I. It is noted that forces due to the moving walls and the buoyancy forces act in the opposite directions in case I. At Ri = 0.1, where forced convection is dominant, for Ar = 1 and 4, a primary recirculation zone is formed, while for Ar = 0.25, two recirculation zones are created within the enclosure with its core being near the lid walls.

Table 2. Thermophysical properties of water and copper.

Property	Fluid phase (water)	Solid phase (Cu)
Cp	4179	383
P	997. 1	8954
K	0.6	400
B	2.1×10^{-4}	1.67×10^{-5}

At Ri = 1, where the natural convection is comparable with forced convection, streamlines show that the forced convection is significant for Ar<4, while free convection is prominent for Ar = 4. For Ar<4, in addition to two recirculation zones formed near lid walls, a recirculation cell in mid-zone of enclosure is also formed due to strengthening of free convection. At Ri = 10, the streamlines show that free convection is predominant. Two thin cells are shaped near the lid walls, while a primary recirculation zone is shaped in mid-zone of the enclosure. The comparison between pattern of streamlines for base fluid and nanofluid shows slight differences.

The isotherm patterns for Ri = 0.1 show that the thermal boundary layer formed near isothermal walls is thinner for higher Ar and therefore, the temperature gradient is significant for higher Ar. It indicates that the forced convection which is dominant in low Ri gives better heat transfer in higher Ar. Such high temperature gradient is also found for Ar = 4 and Ri = 1 which shows forced convection is strength compared to free convection. These temperature gradients in two latest cases are mainly found near top of the hot and bottom of the cold walls.

Due to strengthening of free convection at Ar = 1 and Ri = 1, two slightly dense temperature zones are created where the central recirculation cells are formed. When Ri = 10, free convection is predominant compared to forced convection. At Ar = 4, isotherms clearly show two thermal boundary layer near the isotherm walls. In contrary to the forced convection cases, these gradients are found near bottom of the hot wall and top of the cold wall.

Fig. 5 shows the streamlines and the isotherms for various aspect ratios and Ri numbers for both nanofluid and pure water as the base fluid in case II. It is noted that forces due to the moving lids aid to the buoyancy forces in case II. At Ri = 0.1, where forced convection is dominant, a primary recirculation zone is shaped for Ar>0.25. The axis of the primary cells orients with increasing Ri particularly for Ar = 1 and Ri = 1. For Ar = 0.25, two recirculation zones are shaped near the lid walls, that they extend to the central zone of the enclosure by increasing Ri. This behavior is due to strengthening of free convection forces and aiding effect of forced convection on free convection. Isotherms show that the temperature gradient near the isothermal walls become more sever when Ri decreases especially for Ar>0.25. It is because of increasing the effect of forced convection in heat transfer as a main mechanism of heat transfer. At high Ri, forced convection weakens and thus, heat transfer decreases. Consequently, thermal boundary layers become thicker and thermal layering is formed in central zone of the enclosure.

Fig. 6 and 7 show average Nusselt number (Nuavg) calculated on the hot wall for case I and case II, respectively. By increasing the volume fraction of nanoparticles, Nuavg increases. For Ar = 0.25, the value of Nuavg is less than 1.

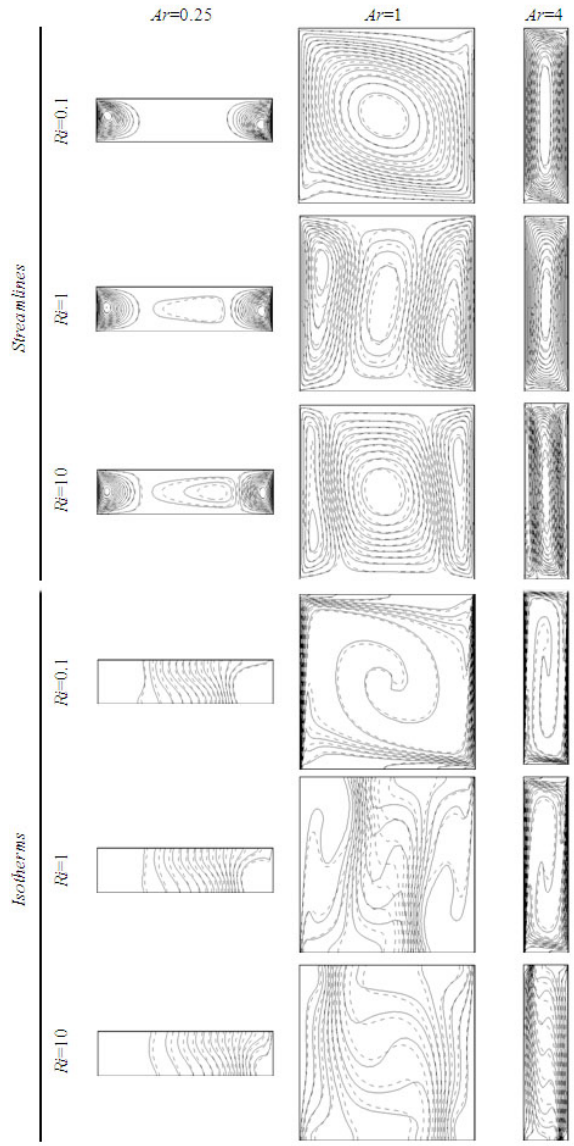

Fig. 4. Streamlines and isotherms for case I with various aspect ratios and Ri (solid lines: pure water and dashed lines: nanofluid with φ=0.08).

By increasing Ar, Nuavg increases due to extending and strengthening recirculation cells. For case I, the value of Nuavg for Ri = 0.1 is more than that of Ri = 10 especially at Ar = 4 where convection strength is significant. This is because of vigorous strength of forced convection at Ri = 0.1 and thus, heat transfer increases. However, free convection heat transfer is dominant at Ri = 10; Nuavg cannot increase as much as that of Ri = 0.1 by increasing volume fraction of nanoparticles. This is not only due to less strength of free convection compared to forced convection, but also opposite effect of forced convection on free convection in case I.

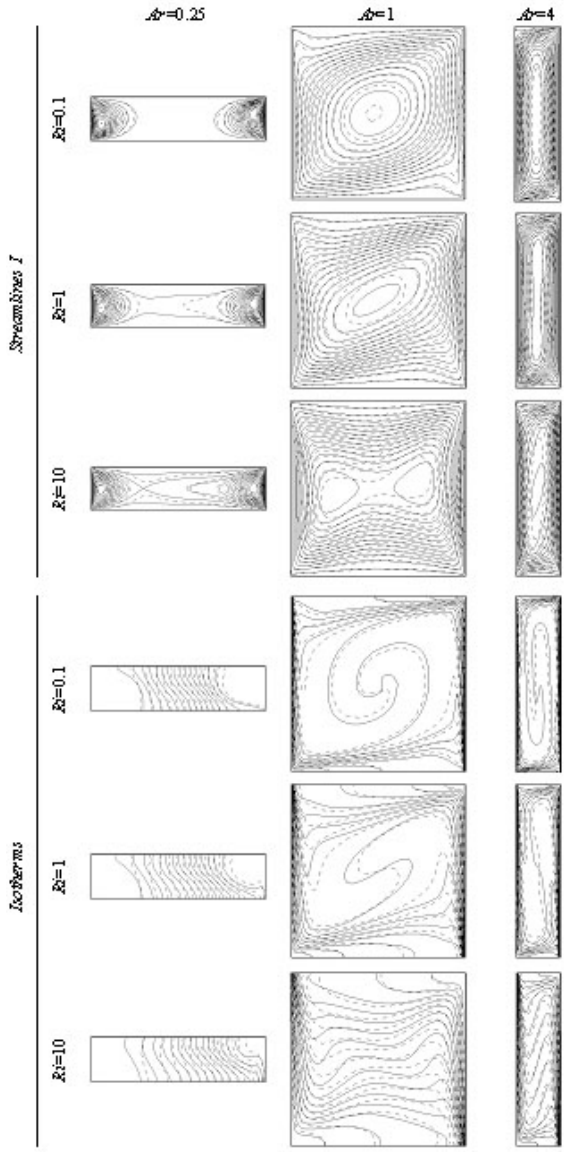

Fig. 5. Streamlines and isotherms for case II with various aspect ratios and Ri (solid lines: pure water and dashed lines: nanofluid with φ=0.08).

For case II, forced convection has an aiding effect on free convection and therefore, at Ri = 10 where free convection is dominant, the value of

Nuavg is more than that of case I. The value of Nuavg for Ri = 0.1 is also more than that of Ri=10 especially at Ar = 4; only exception of that is Ar = 0.25.

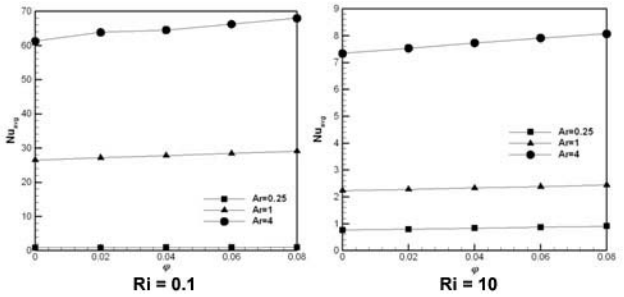

Fig 6. Average Nusselt number on the hot wall versus volume fraction of nanoparticles for various aspect ratios and Ri numbers in case I.

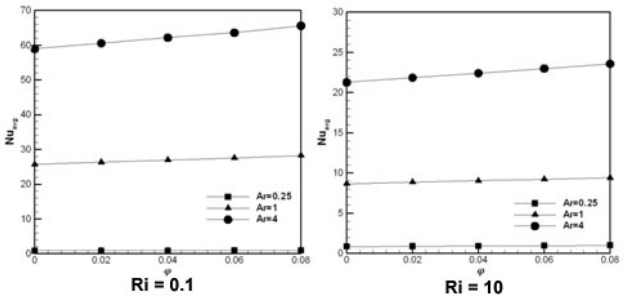

Fig 7. Average Nusselt number on the hot wall versus volume fraction of nanoparticles for various aspect ratios and Ri numbers in case II.

5. Conclusions

In this article, laminar mixed convection is studied in lid-driven enclosures filled with Cu-water nanofluid. Based on the present numerical study, the following results are obtained:

1- The comparison between the patterns of fluid flow and temperature for the nanofluid and the base fluid shows slight differences.

2- When forced convection is dominant, the formed thermal boundary layer near the isothermal walls is thinner for higher Ar and therefore, the temperature gradient is significant that results in better heat transfer.

3- When forced convection is dominant, the temperature gradients are formed near the top of the hot wall and bottom of the cold wall; while, such gradients are found near bottom of the hot wall and top of the cold wall when free convection is dominant.

4- By increasing Ar, Nuavg increases due to extending and strengthening recirculation cells.

5- The variation of average Nusselt number with increasing the volume fraction of nanoparticles, is linear in two cases.

References

[1] U. S. Choi, Enhancing thermal conductivity of fluids with nanoparticles, ASME Fluids Eng. Div. 231 (1995) 99-105.

[2] J.R. Koseff, A.K. Prasad, The lid-driven cavity flow: a synthesis of quantitative and qualitative observations, J. Fluids Eng. Transactions of the ASME106 (1984) 390-398.

[3] M. Morzinski, C.O. Popiel, Laminar heat transfer in a two-dimensional cavity covered by a moving wall, Num. Heat Trans. 12 (1988) 265-273.

[4] W. J. Luo, R. J. Yang, Multiple fluid flow and heat transfer solutions in a two-sided lid-driven cavity, Int. J. Heat Mass Trans. 50 (2007) 2394-2405.

[5] A. M. Al-Amiri, K. M. Khanafer, I. Pop, Numerical simulation of combined thermal and mass transport in a square lid-driven cavity, Int. J. Therm. Sci. 46 (2007) 662-671.

[6] B. Ghasemi, S.M. Aminossadati, Mixed convection in a lid-driven triangular enclosure filled with nanofluids, Int. Commun. Heat Mass Trans. 37 (2010) 1142-1148.

[7] F. Talebi, A. H. Mahmoudi, M. Shahi, Numerical study of mixed convection flows in

a square lid-driven cavity utilizing nanofluid, Int. Commun. Heat Mass Trans. 37 (2010) 79-90.

[8] M.A. Mansour, R.A. Mohamed, M.M. Abd-Elaziz, S. E. Ahmed, Numerical simulation of mixed convection flows in a square lid-driven cavity partially heated from below using nanofluid, Int. Commun. Heat Mass Trans. 37 (2010) 1504-1512.

[9] E. Abu-Nada, A. J. Chamkha, Mixed convection flow in a lid-driven inclined square enclosure filled with a nanofluid, Europ. J. Mech. B/Fluids. 29 (2010) 472-482.

[10] H.C. Brinkman, The viscosity of concentrated suspensions and solutions, J. Chem. Phys. 20 (1952) 571-581.

[11] Y. Xuan, Q. Li, Investigation on convective heat transfer and flow features of nanofluids, ASME J. Heat Trans. 125 (2003) 151-155.

[12] J.C. Maxwell-Garnett, Colours in metal glasses and in metallic films, Philos. Trans. Roy. Soc. A. 203 (1904) 385-342

[13] K. Khanafer, K. Vafai, M. Lightstone, Buoyancy-driven heat transfer enhancement in a two-dimensional enclosure utilizing nanofluids, Int. J. Heat Mass Trans. 46 (2003) 3639-3653.

[14] G. Barakos, E. Mitsoulis, Natural convection flow in a square cavity revisited: laminar and turbulent models with wall functions, Int. J. Num. Meth. Fluids. 18 (1994) 695-719.

[15] N.C. Markatos, K.A. Pericleous, Laminar and turbulent natural convection in an enclosed cavity, Int. J. Heat Mass Trans. 27 (1984) 772-775.

[16] G. De Vahl Davis, Natural convection of air in a square cavity, a benchmark numerical solution, Int. J. Num. Meth. Fluids. 3 (1983) 249-264.

[17] T. Fusegi, J.M. Hyun, K. Kuwahara, B. Farouk, A numerical study of three dimensional natural convection in a differentially heated cubical enclosure, Int. J. Heat Mass Trans. 34 (1991) 1543-1557.